Bridging the Annular Mode and North Atlantic Oscillation paradigms

J. M. Castanheira,[1] M. L. R. Liberato,[2] C. A. F. Marques,[1] and H.-F. Graf[3]

Received 30 January 2007; revised 3 May 2007; accepted 3 July 2007; published 4 October 2007.

[1] The annular nature of the leading patterns of the Northern Hemisphere winter extratropical circulation variability is revisited. The analysis relies on principal component analysis (PCA) of tropospheric geopotential height fields and lagged correlations with the stratospheric polar vortex strength and with a proxy of midlatitude tropospheric zonal mean zonal momentum anomalies. Results suggest that two processes, occurring at different times, contribute to the Northern Annular Mode (NAM) spatial structure. Polar vortex anomalies appear to be associated with midlatitude tropospheric zonal mean zonal wind anomalies occurring before the stratospheric anomalies. After the polar vortex anomalies, zonal mean zonal wind anomalies of the same sign are observed in the troposphere at high latitudes. The timescale separation between the two signals is about 2 weeks. It is suggested that the leading tropospheric variability patterns found in the literature represent variability associated with both processes. The tropospheric variability patterns which appear to respond to the polar vortex variability have a hemispheric scale but show a dipolar structure only over the Atlantic basin. The dipole resembles the North Atlantic Oscillation pattern (NAO), but with the node line shifted northward.

Citation: Castanheira, J. M., M. L. R. Liberato, C. A. F. Marques, and H.-F. Graf (2007), Bridging the Annular Mode and North Atlantic Oscillation paradigms, *J. Geophys. Res.*, *112*, D19103, doi:10.1029/2007JD008477.

1. Introduction

[2] The Northern Annular Mode (NAM), obtained as the leading empirical orthogonal function (EOF) of isobaric geopotential fields, accounts for a large fraction of extratropical atmospheric circulation variability [*Thompson and Wallace*, 1998; *Baldwin and Dunkerton*, 1999; *Quadrelli and Wallace*, 2004]. In the troposphere, the NAM is characterized by a seesaw of atmospheric mass between the polar cap and the middle latitudes, mostly over the ocean basins. Although recognizing the prominence of the variability over the ocean basins, *Thompson and Wallace* [1998, 2000] and *Wallace and Thompson* [2002] argued that the dynamical coupling between the stratosphere and troposphere is manifest as vertically coherent variations in the annular modes of extratropical variability, which are characterized by deep, zonally symmetric fluctuations of the geopotential height and zonal wind fields. The statistical connection between the variability of the stratospheric vortex strength (i.e., the leading PC of the geopotential height field at stratospheric isobaric levels) and the leading PCs of the geopotential height field at tropospheric isobaric levels has been argued in favor of the NAM paradigm [*Thompson and Wallace*, 1998; *Baldwin and Dunkerton*, 1999; *Christiansen*, 2001]. However, while in the stratosphere the NAM is simply interpreted as representing the variability of polar vortex strength, in the troposphere the interpretation is much more difficult because of the entangled sources of tropospheric variability. In fact, an EOF analysis may produce zonally symmetric leading patterns even when the dynamics are not particularly zonally coherent on hemispheric length scales [*Ambaum et al.*, 2001; *Gerber and Vallis*, 2005]. As shown by these authors, performing a principal component analysis (PCA) on a variability field dominated by independent dipolar structures, like the North Atlantic Oscillation (NAO) or the North Pacific Oscillation/West Pacific pattern (NPO/WP), one may obtain leading EOF patterns with a high degree of zonal symmetry. *Deser* [2000] analyzed the teleconnectivity of the three centers of the surface NAM (the Arctic Oscillation pattern, AO). She concluded that the correlation between the Pacific and the Azores centers of action is not significant and, therefore, that the AO cannot be viewed as reflecting such a teleconnection. It was suggested that the AO reflects independent teleconnections between the variability over each ocean basin and the variability over the polar cap. These results support the NAO paradigm: The winter extratropical tropospheric circulation variability is dominated by a regional meridional seesaw over the Atlantic basin (the NAO) and a wave train pattern over the Pacific/North America sector (the PNA) [*Ambaum et al.*, 2001].

[3] As it was demonstrated by *North* [1984], individual EOF modes correspond to individual physical modes only in the very limited class of linear dynamical systems, for

[1]Centro de Estudos do Ambiente e do Mar, Department of Physics, University of Aveiro, Aveiro, Portugal.
[2]Department of Physics, University of Trás-os-Montes e Alto Douro, Vila Real, Portugal.
[3]Centre for Atmospheric Science, Department of Geography, University of Cambridge, Cambridge, UK.

0148-0227/07/2007JD008477

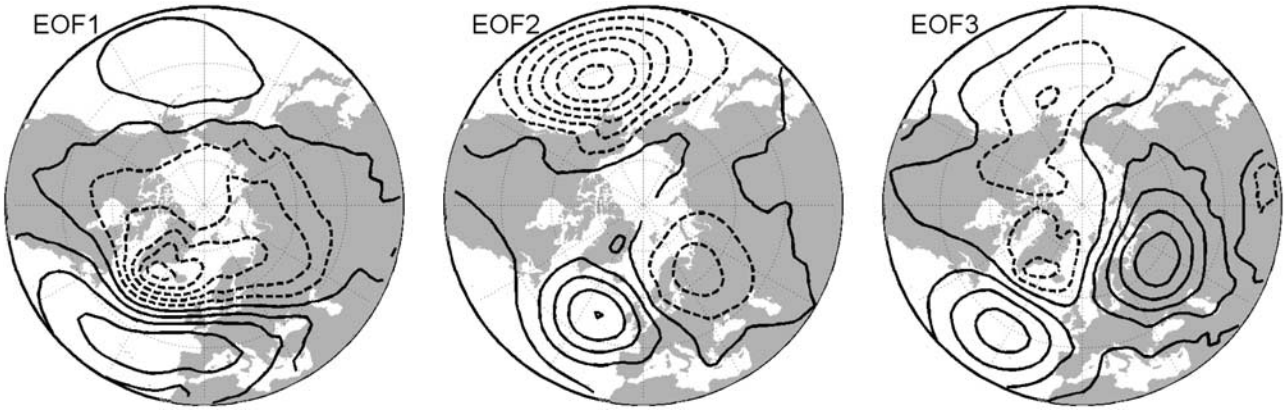

Figure 1. Regression patterns of the 1000-hPa geopotential height on the standardized PCs of 15-days running mean geopotential height anomalies, north of 30°N. EOFs 1, 2 and 3 explain 19.0%, 11.8% and 10.3% of the total variability, respectively. Contour interval is 7.5 gpm, and negative contours are dashed.

which the linear operator commutes with its adjoint. For instance, studying the mean and covariance structure of an idealized zonal jet that fluctuates in strength, position, and width, *Monahan and Fyfe* [2006] obtained analytic results demonstrating that in general the individual EOF modes cannot be interpreted in terms of individual physical processes. The mix of physical processes can be increased when analyzing monthly or seasonal averages, if the processes have smaller timescales and occur sequentially. This may be the case for the daily NAM time series calculated by *Baldwin and Dunkerton* [2001]. These authors projected the daily isobaric geopotential on the leading isobaric EOFs of the seasonal means. However, *McDaniel and Black* [2005] showed that the dynamical processes underlying the annular variability act at the intraseasonal time scale (10–12 days), and *Feldstein and Franzke* [2006] found an *e*-folding timescale of about 10 days for the temporal evolution of both the NAO and NAM indices.

[4] This study discusses the annular nature of the leading isobaric EOFs of the Northern Hemisphere winter extratropical circulation variability. It will be shown that two processes occurring at different times may constitute the NAM spatial structure. The paper is organized as follows: Section 2 describes the data and the methods of analysis. Section 3 presents the obtained results and section 4 makes some concluding remarks.

2. Data and Method

[5] The geopotential height and the zonal wind data used in this study have been obtained from the ECMWF Data Server, ERA-40. Daily means, with 2.5°lat. × 2.5°long. horizontal resolution, for 45 winters (November to March) from 1958 to 2002 were computed. The seasonal cycle was obtained by calculating the time mean for each calendar day followed by a smoothing with a 31-day moving average. Daily anomalies were obtained subtracting the seasonal cycle from the original daily means. A 15-day running mean was applied to the anomalies, in order to filter out shorter timescales. The studied spatial domain is the Northern Hemisphere (NH) extratropical circulation north of 30°N at 1000 hPa and 500 hPa isobaric levels.

[6] The strength of the stratospheric polar vortex is represented by the 50-hPa zonal mean zonal wind at 65°N, here denoted as the $U_{50}(65)$ index. In many studies, the strength of the polar vortex is represented by means of the stratospheric Northern Hemisphere annular mode (NAM) time series as computed by *Baldwin and Dunkerton*

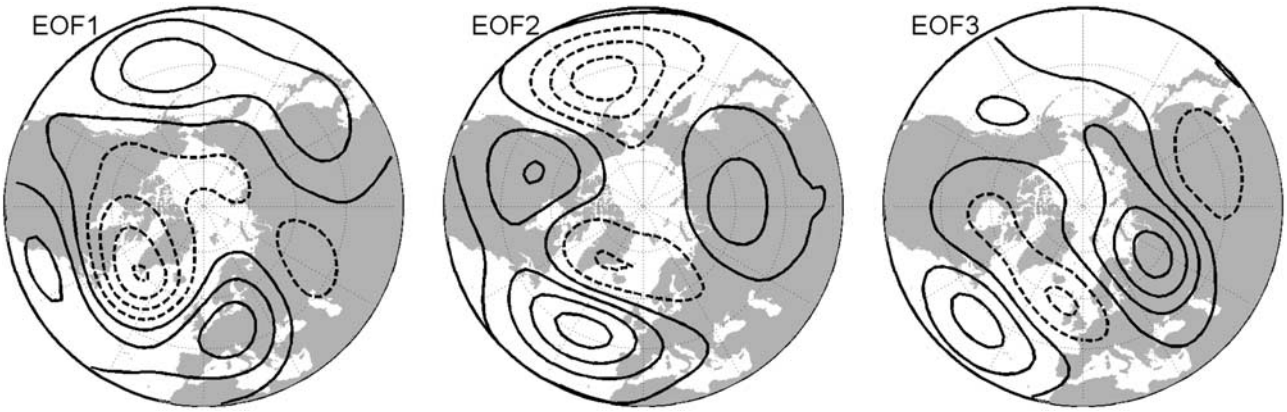

Figure 2. As in Figure 1 but for 500-hPa geopotential height field. EOFs 1, 2 and 3 explain 15.1%, 11.2% and 9.8% of the total variability, respectively. Contour interval is 15 gpm.

Table 1. Correlations Between the First Three PCs of the 1000-hPa Geopotential Height and the First Three PCs of the 500-hPa Geopotential Height[a]

	1000 hPa		
500 hPa	PC1	PC2	PC3
PC1	**0.84**	**−0.41**	0.06
PC2	**0.44**	**0.76**	**0.26**
PC3	−0.08	**−0.20**	**0.67**

[a]Boldface values are above the 99% significance level.

[2001]. Considering the 15-day running means of the NAM index at 50 hPa, obtained from Mark Baldwin's web page (http://www.nwra.com/resumes/baldwin/nam.php), the correlation between this index and the $U_{50}(65)$ index is 0.96. Hence the much simpler zonal mean wind is nearly identical with the 50-hPa NAM index.

[7] A principal component analysis (PCA) was performed on the 1000-hPa and the 500-hPa geopotential height fields. Vertical connection between the obtained patterns and the vortex strength will be assessed by means of lagged correlations between the respective principal components (PCs) and the $U_{50}(65)$ index.

3. Results

3.1. Principal Component Analysis

[8] The leading EOFs of the geopotential height fields at 1000 and 500 hPa are very similar to the ones found in the literature, based on monthly timescales and longer. For the sake of comparison, the first three leading patterns are shown in Figures 1 and 2, for the 1000 hPa and 500 hPa, respectively. The sampling errors of the eigenvalues, according to North's Rule of Thumb, were calculated taking into consideration the time series autocorrelation. Only the first EOF is well separated in both fields. Although statistically distinct, the first EOFs are not necessarily physical modes. It is also worth to note that it makes no difference for the leading EOF structures to chose the spatial domain to be the NH extratropical circulation north of 30°N, as done here, or including lower latitudes from 20°N as in the works of *Thompson and Wallace* [1998, 2000] and others.

[9] Table 1 shows a strong correlation between the same order PCs of the 500-hPa and 1000-hPa geopotential fields. Significant correlation is also observed between the first and second PCs and between the second and the third PCs, indicating some dependence on the represented variabilities.

Table 2. Lagged Correlations Between the First Three PCs of the 1000-hPa (500-hPa) Geopotential Height and the 50 hPa Zonal Mean Zonal Wind at 65°N ($U_{50}(65)$)[a]

	PC1	PC2	PC3
1000 hPa	$\mathbf{0.53}_{(2)}$	$-0.11_{(30)}$	$-0.20_{(-30)}$
500 hPa	$\mathbf{0.47}_{(-2)}$	$\mathbf{0.28}_{(6)}$	$-0.12_{(-13)}$
$\lvert U_{50}\rvert \geq \sigma$, 1000 hPa	$\mathbf{0.73}_{(1)}$	$0.18_{(12)}$	$0.24_{(10)}$
$\lvert U_{50}\rvert \geq \sigma$, 500 hPa	$\mathbf{0.67}_{(-4)}$	$\mathbf{0.51}_{(6)}$	$0.15_{(-30)}$

[a]Shown are the lagged correlations with maximum absolute values, and the numbers in parentheses indicate the lag in days for their occurrence. Positive lags mean that the stratosphere is leading. Boldface values are above the 99% significance level. The last two rows are similar to the first two rows but considering only $U_{50}(65)$ anomalies above or below one standard deviation.

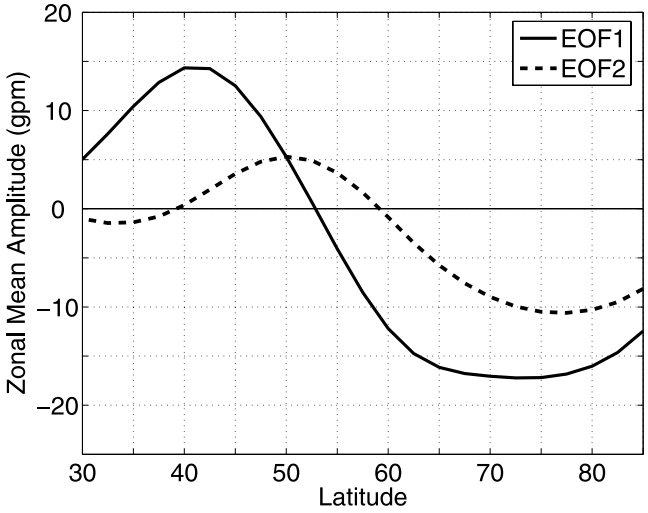

Figure 3. Meridional profiles of the zonal mean amplitude of the first (solid line) and second (dashed line) EOFs of the 500-hPa geopotential height variability. The amplitudes were normalized to one standard deviation of the respective PCs.

The significance levels were calculated by means of 10,000 random permutations of the years preserving the serial autocorrelation.

[10] The statistical connection between the tropospheric variability and the stratospheric annular variability is assessed calculating the lagged correlations of the tropospheric PCs with the 50 hPa zonal mean zonal wind at 65°N, the $U_{50}(65)$ index. Table 2 shows the lagged correlations with maximum absolute value and the lags of occurrence. Positive lags mean that the stratospheric wind is leading. As expected from other works [e.g., *Baldwin and Dunkerton*, 2001], the leading PCs of the tropospheric variability show significant correlations with the stratospheric vortex strength. Also worth to note is the smaller but significant correlation between the stratospheric vortex strength and the second PC of the 500-hPa geopotential height. This shows that the leading PC of the 500 hPa geopotential height (the NAM index [*Baldwin and Dunkerton*, 2001]) does not represent the full linear connection between the midtroposphere circulation and the stratospheric vortex strength. *Christiansen* [2002] also argued the importance of the second EOF for the statistical connection with the stratospheric vortex.

[11] To obtain some insight into the origin of the correlations between the $U_{50}(65)$ index and the first two 500-hPa PCs, we analyzed the annularity of the respective EOF patterns. Figure 3 shows the meridional profiles of the zonal mean amplitude of the two first 500-hPa EOFs patterns. Using the geostrophic balance, the zonal mean zonal wind anomalies associated with each PC are proportional to the slopes of the meridional profiles of the zonal mean amplitude of the respective EOF patterns. From Figure 3, it may be concluded that EOF1 is associated with strong zonal mean zonal wind variability in the latitudinal belt 45°N to 65°N, whereas EOF2 is associated with a zonal mean zonal wind variability at higher latitudes between 55°N and 70°N.

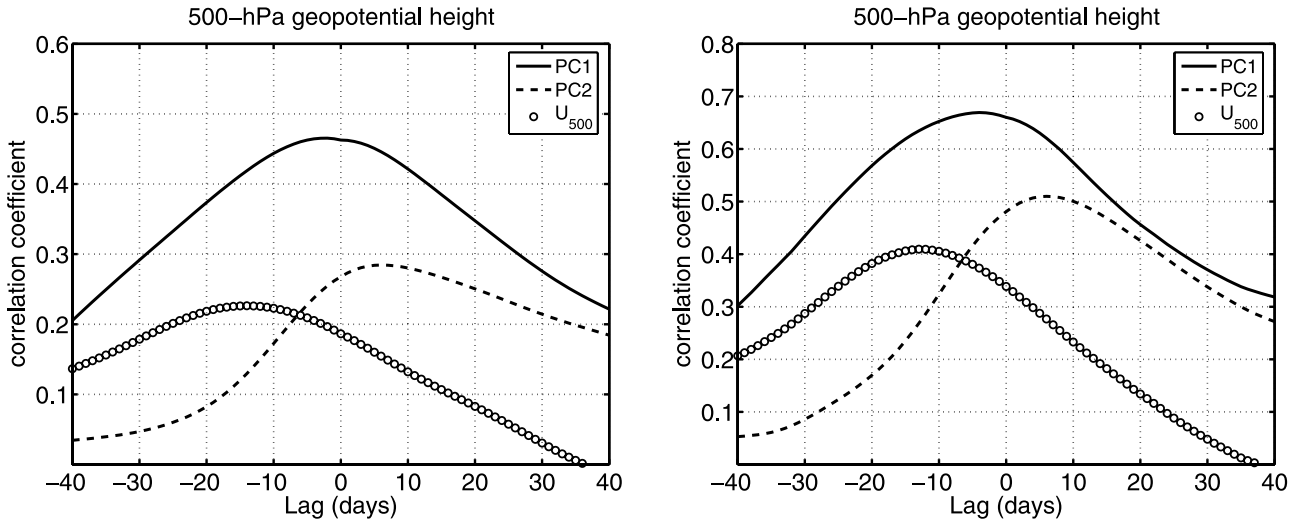

Figure 4. Lagged correlations between the 50-hPa zonal mean zonal wind at 65°N ($U_{50}(65)$) and the first two PCs of the 500-hPa geopotential height fields. The curve U_{500} represents the lagged correlation between the $U_{50}(65)$ index and the 500-hPa zonal mean zonal wind in the latitudinal belt 45–55°N. The right plot is similar to the left one but considering only $U_{50}(65)$ anomalies above or below one standard deviation. Positive lags mean that the stratospheric wind is leading.

EOF2 does not explain any variability of the zonal mean zonal wind around 50°N.

[12] To see if the variability of the zonal mean zonal wind around 50°N is contributing to the higher correlation between the 500-hPa PC1 and the vortex strength, we calculated the 500-hPa zonal mean zonal wind anomaly averaged in the latitudinal band 45–55°N. This time series will be designated as $U_{500}(45-55)$ index. The lagged correlations between $U_{500}(45-55)$ and $U_{50}(65)$ are shown in Figure 4. The maximum correlation (r = 0.23) between $U_{500}(45-55)$ and $U_{50}(65)$ is statistically significant at the 99% level and occurs when the $U_{500}(45-55)$ index is leading by 14 days. If one considers only vortex anomalies above or below one standard deviation, the maximum correlation is 0.41 with the index $U_{500}(45-55)$ leading by 13 days. The lagged correlation of the vortex strength with $U_{500}(45-55)$ and PC2 (Figure 4) suggests that there are processes occurring at different times: First, zonal mean wind anomalies in the midlatitude troposphere lead stratospheric polar vortex anomalies of the same sign. Once these are established, the positive correlations with PC2 indicate that stratospheric vortex strength anomalies are leading higher-latitude tropospheric zonal mean wind anomalies of the same sign by few days. The positive correlations between $U_{500}(45-55)$ and $U_{50}(65)$ are consistent with the lagged cross correlation between the 300-hPa NAM and the 300-hPa zonally averaged momentum flux poleward of 20N calculated by *Baldwin et al.* [2003]. As shown by *Baldwin et al.* [2003, Figure 4a], the correlations are higher when the upper tropospheric momentum flux anomalies lead the NAM anomalies. *McDaniel and Black* [2005, Figure 4c] also shows significant poleward eddy momentum flux anomalies at midlatitude upper troposphere/lower stratosphere, during the maturing stage of strong positive NAM events. Hence our interpretation of the correlations in Figure 4 is that the initial zonal mean momentum anomalies are shifted to the high latitudes by zonal mean-eddy interactions leading to vortex anomalies of the same sign.

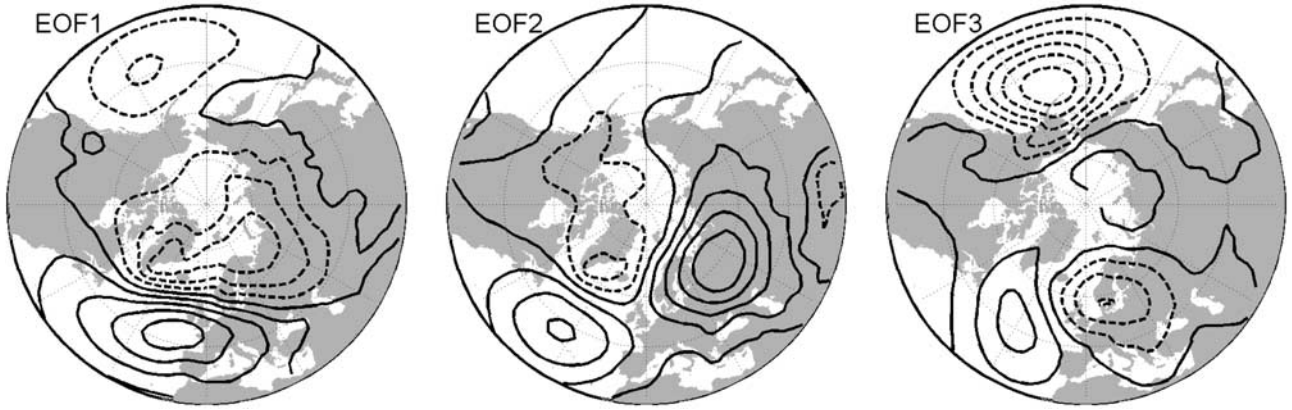

Figure 5. As in Figure 1 but for the residual geopotential height variability. EOFs 1, 2 and 3 explain 17.7%, 11.8% and 11.4% of the 1000-hPa residual variability, respectively.

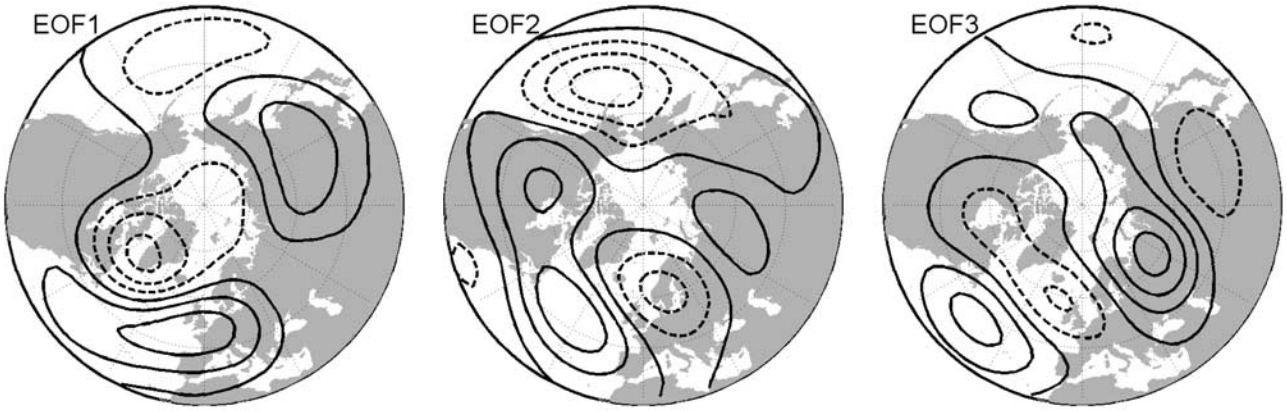

Figure 6. As in Figure 2 but for the residual geopotential height variability. EOFs 1, 2 and 3 explain 13.5%, 13.1% and 11.6% of the 500-hPa residual variability, respectively.

Then the vortex anomalies will progress downward affecting back the high-latitude troposphere.

[13] The correlation between the $U_{50}(65)$ index and the PC1 is higher and shows a maximum at a lag shorter than the ones for the maxima of the correlations with the PC2 and $U_{500}(45-55)$ index. The fact that the maximum correlation between the $U_{50}(65)$ index and the PC1 occurs at negative lags does not support the idea of a downward influence of the stratospheric vortex variability. However, this contradiction may be a consequence of the PCA methodology. The criterion for the identification of the leading EOF/PC is only the maximization of the explained data variability. The more are the variability processes projected onto the leading EOF the greater is the explained variability by the leading PC. The blend of processes may be favored by the use of 15-days running mean low-pass filtering of the time series. In fact, the 500-hPa PC1 correlates both with $U_{50}(65)$ (r_{max} = 0.47 at lag −2) and with $U_{500}(45-55)$ (r_{max} = 0.64 at lag −1) indices, whereas the 500-hPa PC2 does not show any correlation with $U_{500}(45-55)$ (r_{max} = 0.07).

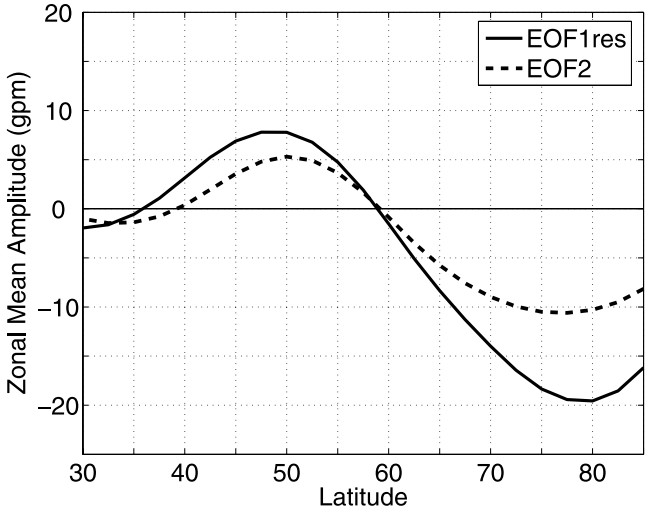

Figure 7. Meridional profiles of the zonal mean amplitude of the first EOF of the residual 500-hPa geopotential height variability (solid line) and second EOF of the total 500-hPa geopotential height variability (dashed line). The amplitudes are normalized to one standard deviation of the respective PCs.

3.2. PCA of the Residual Fields

[14] To separate the two processes discussed above, the geopotential height fields were linearly regressed on the $U_{500}(45-55)$ index. Residual geopotential height fields were defined as the geopotential height field minus the variability linearly regressed on the $U_{500}(45-55)$ index. Then, we performed a PCA of the residual geopotential fields, and recalculated the lagged correlation as in the previous subsection.

[15] The first 3 EOFs of the residual geopotential height fields are shown in Figures 5 and 6, for the 1000 hPa and 500 hPa, respectively. Using the geostrophic balance, it may be deduced from Figure 7 that the leading EOF of the 500-hPa residual variability represents anomalies of the zonal mean zonal wind at the same latitudinal band as the second EOF of the total variability, but the anomalies are stronger. The zonal mean geopotential height anomalies show a maximum centered at 50°N. Hence, as expected the leading EOF pattern of the residual data does not represent any wind anomaly around 50°N.

[16] The leading EOFs of the residual variability at 1000 hPa and 500 hPa (Figures 5 and 6) show midlatitude centers of opposite sign over the North Atlantic and North Pacific, whereas the respective EOF1s of the total variability (Figures 1 and 2) have two centers of equal polarity, which are taken as an expression of the annularity. The leading EOFs of the residual variability only show a meridional dipole over the Atlantic basin resembling the NAO, but with the node line shifted northward. Table 3 shows the corre-

Table 3. As in Table 1 but for the Residual Geopotential Height Variability[a]

	1000 hPa		
500 hPa	PC1	PC3	PC2
PC1	**0.92**	−0.04	**0.18**
PC2	0.12	**0.81**	0.02
PC3	−0.15	0.15	**0.66**

[a]Note that the order of the 1000-hPa PC2 and PC3 was changed in the table.

Table 4. As in Table 2 but for the Residual Geopotential Height Variability

	PC1	PC2	PC3
1000 hPa	**0.53**$_{(7)}$	0.16$_{(15)}$	−0.19$_{(8)}$
500 hPa	**0.51**$_{(4)}$	−0.17$_{(-20)}$	−0.10$_{(13)}$
$\|U_{50}\| \geq \sigma$, 1000 hPa	**0.73**$_{(7)}$	0.28$_{(9)}$	−0.23$_{(-10)}$
$\|U_{50}\| \geq \sigma$, 500 hPa	**0.73**$_{(5)}$	−0.24$_{(-25)}$	−0.10$_{(-14)}$

lation between the PCs of the 500-hPa and 1000-hPa residual geopotential fields. Now, the PCs are paired one to one, and the first two PCs show an increase in correlation when compared with the values obtained for the total variability (Table 1). Note that the order of the second and third PCs of the 1000-hPa residual geopotential field are switched in Table 3. The variances of PC2 and PC3 are very close and their order may be changed because of noise. In fact, the EOF patterns associated with PC2 and PC3 of the residual variability (Figure 5) are very close to the EOF patterns associated with PC3 and PC2 of the total variability (Figure 1), respectively.

[17] The correlation between the first 3 PCs of the residual variability and the vortex strength are shown in Table 4. Now, only the leading PCs show statistically significant correlation with the vortex strength and the correlation maxima at both isobaric levels occur at positive lags and have close values. The curves of lagged correlations (Figures 8 and 9) are consistent with a delayed downward influence of the stratospheric vortex on the residual tropospheric variability. However, when considering the total variability, the maximum of correlation between the leading PC of 500-hPa geopotential height and the vortex strength occurs for negative lags, i.e., with the tropospheric variability leading (Figure 4). These results suggest that, after removing the variability linearly dependent on the $U_{500}(45-55)$ index, the leading EOFs/PCs of the residual variability capture mainly the downward influence of the stratospheric vortex variability.

[18] Until now, all the lagged correlations were based in daily time series smoothed by a 15-day running mean. It is of interest to assess the effect of the smoothing on the lags. Lagged correlations as the ones showed in Figure 4 were recalculated using unfiltered (i.e., not averaged) daily time series (Figure 10a). Unfiltered time series for PC1 and PC2 were obtained projecting the daily unfiltered anomalies onto the EOF1 and EOF2 of the 500-hPa geopotential height field smoothed by the 15-day running mean. Figure 10a shows the same lag features as those observed in Figure 4. The curve representing the lagged correlations between the unfiltered time series of PC1 and the vortex strength shows a maximum near to zero lag and shoulder for negative lags. The maximum and the shoulder suggest, now more clearly, that the processes underlying the correlation of the $U_{500}(45-55)$ index and the PC2 with the vortex strength may be associated with circulation variability which projects also on the EOF1.

[19] The time separation between the two signals is also clear if we consider only the intraseasonal variability, i.e., the variability which remains after removing the seasonal (November to March) means. Figure 10b summarizes the main findings of this study. Figure 10b represents the lagged correlations between the intraseasonal anomalies of the $U_{50}(65)$ index and the intraseasonal anomalies of the first two PCs of the 500-hPa total geopotential height variability, the $U_{500}(45-55)$ index, and the leading PC of the 500-hPa residual geopotential height variability. Only $U_{50}(65)$ anomalies above or below one standard deviation of the intraseasonal variability were considered.

4. Concluding Remarks

[20] This study discussed the annular nature of the leading isobaric EOFs of the Northern Hemisphere winter extratropical circulation variability. The obtained results suggest that two processes, occurring at different times, may contribute to the NAM spatial structure. Polar vortex

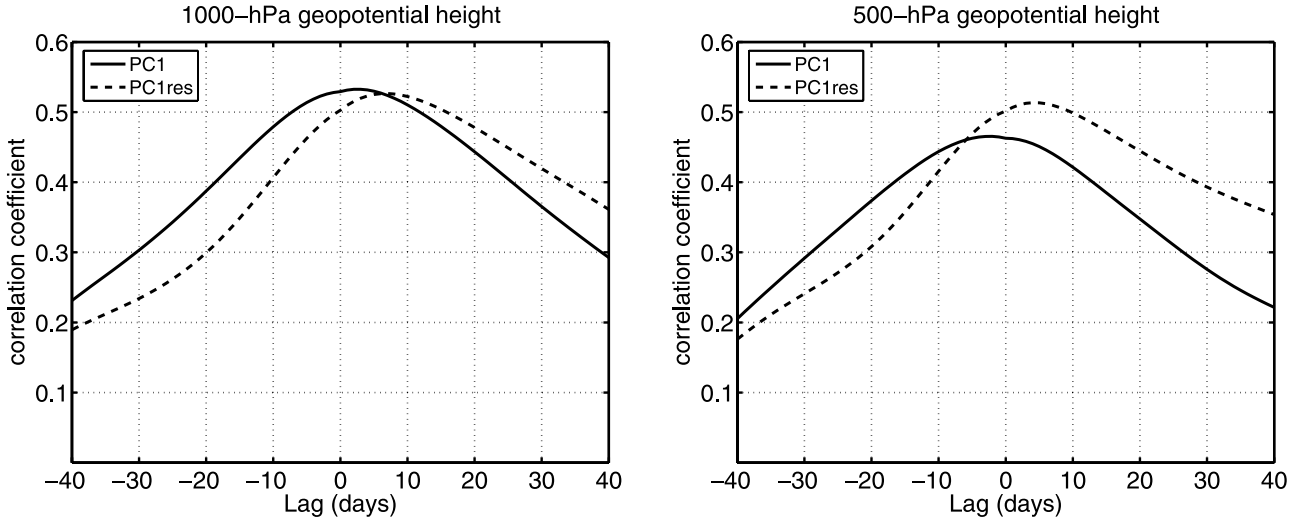

Figure 8. Lagged correlations between the 50-hPa zonal mean zonal wind at 65°N and the leading PCs of the total (solid line) and residual (dashed line) variabilities of (left) 1000-hPa and (right) 500-hPa geopotential height fields. Positive lags mean that the stratospheric wind is leading.

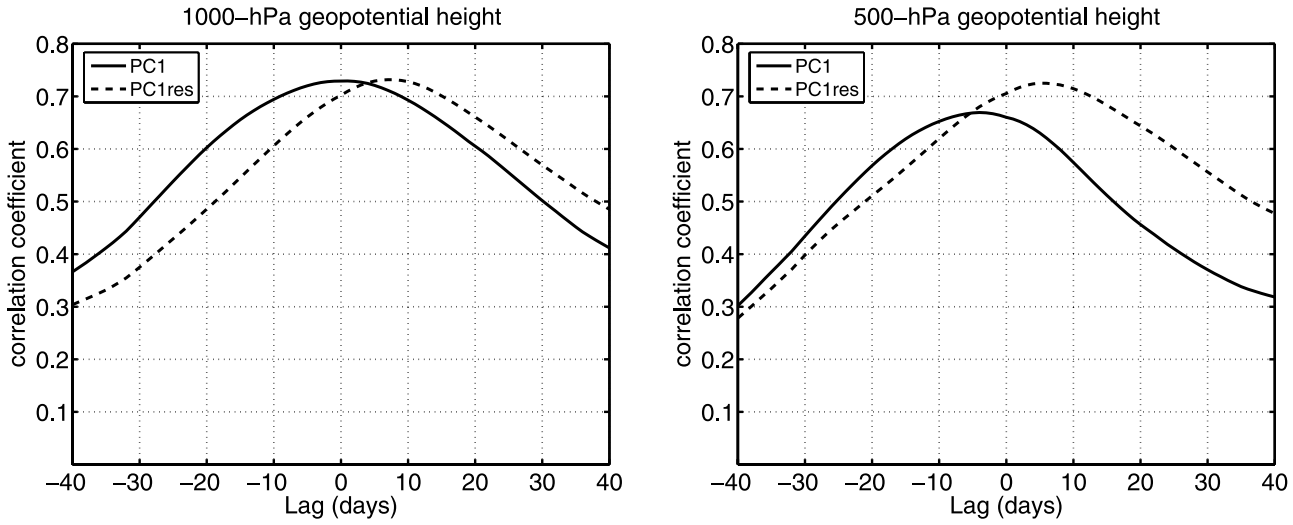

Figure 9. As in Figure 8 but considering only 50-hPa zonal mean zonal wind anomalies above or below one standard deviation.

anomalies appear positively correlated with midlatitude tropospheric zonal mean zonal wind anomalies occurring before the stratospheric anomalies. Following the polar vortex anomalies zonal mean zonal wind anomalies of the same sign are observed in the troposphere at high latitudes. The timescale separation of the two signals is of about 2 weeks (Figures 4 and 10a). In a PCA the criterion for the identification of the leading PC is the maximization of the explained data variability. Results suggest that, in the case of tropospheric circulation, this maximization is achieved with the variability associated with the two above processes projecting on the leading EOF pattern. The "accumulation" or "deficit" of zonal mean zonal momentum at midlatitudes confers the annular character to the leading patterns in those latitudes, and the "response" to vortex variability confers the annularity at high latitudes.

[21] Finally, it is worth remarking that subtracting the variability linearly dependent on the $U_{500}(45-55)$ index does not necessarily mean removing a dynamical zonally symmetric component. In fact, the correlation between the time series of the midlatitude (45–55°N) zonal wind strengths over the East Asia/Pacific sector (120°E, 240°E) and over the Atlantic sector (90°W, 40°E) is very close to zero ($r = 0.02$). On the other hand, the leading EOF patterns of the residual variability, which seem to respond to the vortex variability have a hemispheric scale but only show a dipolar structure over the Atlantic basin like the NAO. These findings agree with the results of *Feldstein and Franzke* [2006] which suggest that nor the NAO events are confined to the North Atlantic, nor NAM events are annular.

[22] The separation of the two processes that contribute for the tropospheric NAM is important in studies of the tropospheric response to changes originated in the stratosphere, e.g., changes in stratospheric chemical composition. The NAM indices represent zonal symmetric zonal wind

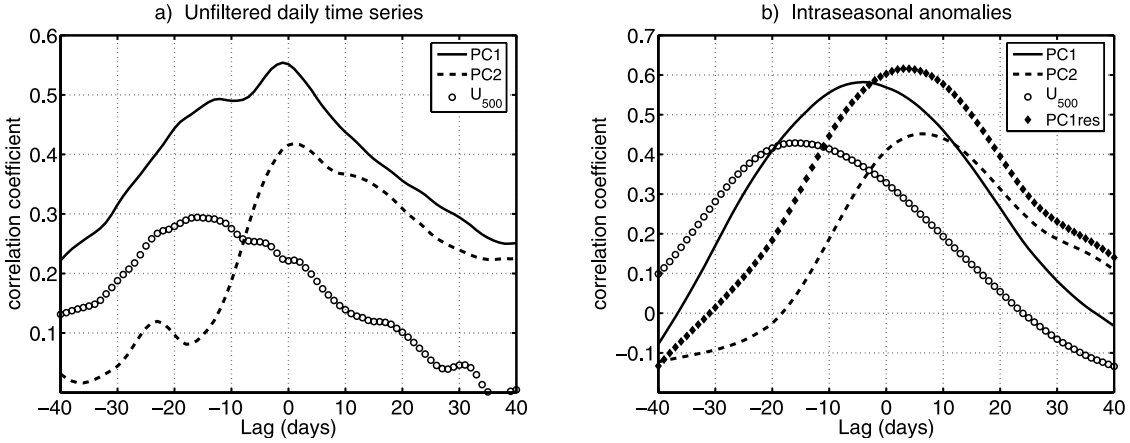

Figure 10. As Figure 4 (right) but (a) considering unfiltered (i.e., not averaged) time series and (b) considering only the intraseasonal variability. The curve PC1res represents the lagged correlation between the $U_{50}(65)$ index and the leading PC of the 500-hPa geopotential height residual variability.

anomalies which spread from middle latitudes to high latitudes, whereas the annularity of tropospheric response to stratospheric anomalies is confined to high latitudes only.

[23] **Acknowledgments.** Margarida L. R. Liberato appreciates the grant SFRH/BD/32640/2006 she received from the FCT (Fundação para a Ciência e a Tecnologia, Portugal).

References

Ambaum, M. H. P., B. J. Hoskins, and D. B. Stephenson (2001), Arctic Oscillation or North Atlantic Oscillation?, *J. Clim.*, *14*, 3495–3507.

Baldwin, M. P., and T. J. Dunkerton (1999), Propagation of the Arctic Oscillation from the stratosphere to the troposphere, *J. Geophys. Res.*, *104*(D24), 30,937–30,946.

Baldwin, M. P., and T. J. Dunkerton (2001), Stratospheric harbingers of anomalous weather regimes, *Science*, *294*, 581–584.

Baldwin, M. P., D. B. Stephenson, D. W. J. Thompson, T. J. Dunkerton, A. J. Charlton, and A. ONeill (2003), Stratospheric memory and skill of extended-range weather forecasts, *Science*, *301*, 636–640.

Christiansen, B. (2001), Downward propagation of zonal mean zonal wind anomalies from the stratosphere to the troposphere: Model and reanalysis, *J. Geophys. Res.*, *106*, 27,307–27,322.

Christiansen, B. (2002), On the physical nature of the Arctic Oscillation, *Geophys. Res. Lett.*, *29*(16), 1805, doi:10.1029/2002GL015208.

Deser, C. (2000), On the teleconnectivity of the "Arctic Oscillation," *Geophys. Res. Lett.*, *27*, 779–782.

Feldstein, S. B., and C. Franzke (2006), Are the North Atlantic Oscillation and the Northern Annular Mode distinguishable?, *J. Atmos. Sci.*, *63*, 2915–2930.

Gerber, E. P., and G. K. Vallis (2005), A stochastic model for the spatial structure of annular pattern of variability and the North Atlantic Oscillation, *J. Clim.*, *18*, 2102–2118.

McDaniel, B. A., and R. X. Black (2005), Intraseasonal Dynamical evolution of the Northern Annular Mode, *J. Clim.*, *18*, 3820–3839.

Monahan, A. H., and J. C. Fyfe (2006), On the nature of zonal jet EOFs, *J. Clim.*, *19*, 6409–6424.

North, G. R. (1984), Empirical orthogonal functions and normal modes, *J. Atmos. Sci.*, *41*, 879–887.

Quadrelli, R., and J. M. Wallace (2004), A simplified linear framework for interpreting patterns of Northern Hemisphere wintertime variability, *J. Clim.*, *17*, 3728–3742.

Thompson, D. W., and J. M. Wallace (1998), The Arctic Oscillation signature in the wintertime geoptential height and temperature fields, *Geophys. Res. Lett.*, *25*, 1297–1300.

Thompson, D. W., and J. M. Wallace (2000), Annular modes in the extratropical circulation, Part I: Month-to-month variability, *J. Clim.*, *13*, 1000–1016.

Wallace, J. M., and D. W. J. Thompson (2002), The Pacific center of action of the Northern Hemisphere Annular Mode: Real or artifact?, *J. Clim.*, *15*, 1987–1991.

J. M. Castanheira, Centro de Estudos do Ambiente e do Mar, Department of Physics, University of Aveiro, 3810-193 Aveiro, Portugal. (jcast@ua.pt)

H.-F. Graf, Centre for Atmospheric Science, Department of Geography, University of Cambridge, Cambridge CB2 3EN, UK. (hfg21@cam.ac.uk)

M. L. R. Liberato, Department of Physics, University of Trás-os-Montes e Alto Douro, 5001-911 Vila Real, Portugal. (mlr@utad.pt)

C. A. F. Marques, Department of Physics, University of Aveiro, 3810-193 Aveiro, Portugal. (cfernandes@fis.ua.pt)